

**Project Summary - Grant # 47589-CH**  
**(Reporting Period: May 2005 – April 2008)**

**Fundamental Investigations of Durability at a Polymer Electrolyte-Electrode Interface**

PI Name: Professor Sanjeev Mukerjee  
Department: Chemistry and Chemical Biology  
Institution, City, State, Zip: Northeastern University, Boston, MA 02115

**Objective**

The overall objectives of this proposed effort was to further our fundamental understanding of degradation pathways at a polymer electrolyte-electrode interface. Towards this goal the key thrust areas proposed in this project were:

- (1) Understanding the role of peroxide lead free radical attack on the polymer electrolyte at the interface with both anode and cathode electrodes using a specially designed PEM cell enabling accelerated degradation conditions simulating practical H<sub>2</sub>/Air PEM operation. In this effort the correlation was made with peroxide yield measured directly using RRDE methods with concomitant degradation of the membrane and ionomer.
- (2) Understanding the effect of Ru stability in a variety of PtRu electrocatalysts under various DMFC operating conditions and the effect of its migration and deposition at the cathode. A combination of fuel cell studies and rotating disk electrode method are used to quantify the losses at both anode and cathode electrodes, these are correlated with the nature of the PtRu/C bulk and surface properties.
- (3) Understanding the effect of alloying on the stability of cathode electrocatalysts under various fuel cell operating conditions, especially at open circuit conditions.

**Approach:**

- (1) Tailored synthesis of electrocatalysts for probing specific aspects of electrocatalyst degradation. These include micellar methods for preparation of monodispersed crystallites with both homogeneous and core shell structures.
- (2) Application of in situ advanced synchrotron based x-ray absorption methods for investigating changes to the short range atomic order and site specific adsorption modes on transition metal surfaces. Specific aspects of corrosion, dissolution surface segregation were probed as a function of various PEM fuel cell operating conditions.
- (3) Specifically designed accelerated durability protocols were established using a unique segmented cell set up. This allowed for probing polymer electrolyte stability at the interface with both anode and cathode electrodes. Correlation with other standard techniques such as RRDE, step scan IR studies etc. were used to complete our understanding of the specific degradation process.

**Relevance to Army**

Understanding durability from the perspective of materials preparation, morphology, bulk and surface characteristic are designed to provide the Army with benchmarks for various devices under consideration for future combat missions and soldier power. Such understanding is expected to show the way towards more active and stable choice of materials and provide the window of operation to ensure long term reliability.

Report Documentation Page				Form Approved OMB No. 0704-0188	
Public reporting burden for the collection of information is estimated to average 1 hour per response, including the time for reviewing instructions, searching existing data sources, gathering and maintaining the data needed, and completing and reviewing the collection of information. Send comments regarding this burden estimate or any other aspect of this collection of information, including suggestions for reducing this burden, to Washington Headquarters Services, Directorate for Information Operations and Reports, 1215 Jefferson Davis Highway, Suite 1204, Arlington VA 22202-4302. Respondents should be aware that notwithstanding any other provision of law, no person shall be subject to a penalty for failing to comply with a collection of information if it does not display a currently valid OMB control number.					
1. REPORT DATE <b>2008</b>		2. REPORT TYPE		3. DATES COVERED <b>00-00-2005 to 00-00-2008</b>	
4. TITLE AND SUBTITLE <b>Fundamental Investigations of Durability at a Polymer Electrolyte-Electrode Interface</b>				5a. CONTRACT NUMBER	
				5b. GRANT NUMBER	
				5c. PROGRAM ELEMENT NUMBER	
6. AUTHOR(S)				5d. PROJECT NUMBER	
				5e. TASK NUMBER	
				5f. WORK UNIT NUMBER	
7. PERFORMING ORGANIZATION NAME(S) AND ADDRESS(ES) <b>Department of Chemistry and Chemical Biology Institution, Northeastern University, Boston, MA, 02115</b>				8. PERFORMING ORGANIZATION REPORT NUMBER <b>; 47589.1</b>	
9. SPONSORING/MONITORING AGENCY NAME(S) AND ADDRESS(ES) <b>U.S. Army Research Office, P.O. Box 12211, Research Triangle Park, NC, 27709-2211</b>				10. SPONSOR/MONITOR'S ACRONYM(S)	
				11. SPONSOR/MONITOR'S REPORT NUMBER(S) <b>47589.1</b>	
12. DISTRIBUTION/AVAILABILITY STATEMENT <b>Approved for public release; distribution unlimited</b>					
13. SUPPLEMENTARY NOTES					
14. ABSTRACT					
15. SUBJECT TERMS					
16. SECURITY CLASSIFICATION OF:			17. LIMITATION OF ABSTRACT <b>Same as Report (SAR)</b>	18. NUMBER OF PAGES <b>9</b>	19a. NAME OF RESPONSIBLE PERSON
a. REPORT <b>unclassified</b>	b. ABSTRACT <b>unclassified</b>	c. THIS PAGE <b>unclassified</b>			

## Accomplishments for Reporting Period

- Correlation with catalyst bulk and surface characteristics with corresponding peroxide yield.
- Validation of accelerated test methodology for correlation of peroxide yields and interfacial stability of the membrane.
- Understanding the effect of Ru migration at the cathode electrode in a DMFCs and the evolution of materials consideration for a stable PtRu anode.
- Fundamental understanding of Pt surface poisoning from halide ions.

## Collaborations and Technology Transfer

- Establishment of collaborative efforts with catalyst vendors, these include BASF-ETEK, and Cabot-Superior Micropowders.
- Establishment of joint efforts for understanding interfacial stability of perfluorinated membranes and ionomers with W. L. Gore, BASF and Advent N.A.
- Understanding durability for specific device considerations with Encite llc.
- Development of Ultra-stable PtRu Electrocatalysts.

These are to translate the results of this research to the industry and incorporation into actual devices.

## Resulting Journal Publications During Reporting Period (May 2005 onwards)

- (1) 'Investigation of Durability Issues of Selected Nonfluorinated Proton Exchange Membranes for Fuel Cell Applications', L. Zhang and S. Mukerjee, *J. Electrochem. Soc.*, **153**, A 1062
- (2) 'CO Coverage/Oxidation Correlated with PtRu Electrocatalyst Particle Morphology in 0.3 M Methanol by in situ XAS', F. Scott, D. Ramaker and S. Mukerjee, *J. Electrochem. Soc.*, **154**, A 396 (2007).
- (3) Specific vs. Non Specific Absorption of Anions on Pt and Pt based Alloys, M. Teliska, S. Mukerjee and D. Ramaker, *J. Phys. Chem. C*, **111**, 9267 (2007)
- (4) 'The Impact of Ru Contamination of a Pt/C Electrocatalyst on Its Oxygen Reduction Activity', L. Gancs, B. Hult, N. Hakim and S. Mukerjee, *Electrochem. Sol. St. Lett.*, **10**, B150 (2007)
- (5) 'Degradation Mechanism Study of Perfluorinated Proton Exchange Membrane under Fuel Cell Operating Conditions' N. Ramaswamy, N. Hakim and S. Mukerjee, *Electrochim. Acta*, **53**, 3279 (2008).
- (6) 'Enhanced Activity and Intefacial Stability Study of Ultra-Low Pt based Electrocatalysts Prepared by Ion Beam Assisted Deposition', N. Ramaswamy, T. M. Arruda, W. Wen, N. Hakim, M. Saha, A. Gulla and S. Mukerjee, *Electrochim Acta*, *In Press*
- (7) 'Impact of Ru Dissolution and Migration in a DMFCs Environment' S. Shyam, T. Arruda, D. Ramaker and S. Mukerjee, *J. Phys. Chem.*, (Submitted May 2009)

## Graduate Students Involved

- Lei Zhang (graduate student). Received Ph.D degree in May 2006
- Nagappan Ramaswamy (graduate student)
- Dr. Lajos Gancs (Postdoctoral Research Associate) [Part time support]

## Awards, Honors and Appointments

- Awarded the Klein Memorial Award at Northeastern University, April 2007

# Understanding the Nature of Interfacial Degradation of Polymer Electrolytes due to Peroxide lead Free Radical Attack

Student: Lei Zhang (Graduated May 2006) and Nagappan Ramaswamy (2<sup>nd</sup> year graduate student)

Novel accelerated technique was used to investigate and correlate the peroxide generation at an electrode/electrolyte interface from the perspective of radical initiated perfluorinated membrane degradation as a function of

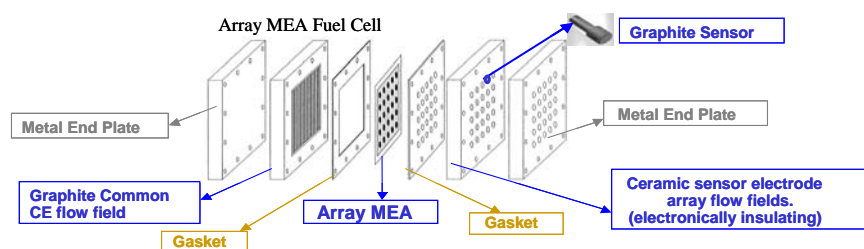


Fig 1: Experimental Setup for Durability Study

cell configurations using a novel segmented cell design (see figure 1 in inset) so that the two formerly

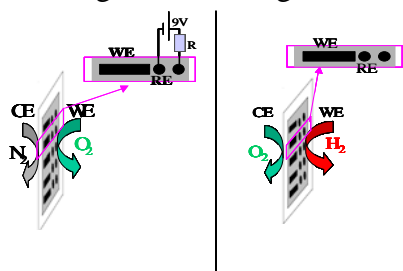


Figure 2. Schematic for evaluating peroxide initiated chemical attack at cathode and anode electrodes respectively in a segmented PEM cell.

proposed PEM degradation mechanisms could be evaluated individually without interference. Details of this methodology are published earlier.<sup>1</sup> Peroxide generation observed on the ring electrode of a RRDE for various electrocatalysts used in this study showed a one-on-one relation with the level of degradation of perfluorinated membrane via local Fenton type reactions at the cathode-membrane interface of an operating fuel cell due to the simultaneous  $2e^-$  pathway of ORR along with the more predominant  $4e^-$  reduction to water.. This is exemplified by tables 1 and 2 wherein the peroxide yields are shown along with the corresponding changes in the proton conductivity

and ion exchange capacity after subjecting the cell to accelerated cathode side condition shown in figure 2 (Lhs).

Catalyst	%H <sub>2</sub> O <sub>2</sub> @0.7V	%H <sub>2</sub> O <sub>2</sub> @0.6V	%H <sub>2</sub> O <sub>2</sub> @0.4V
30% Pt/C	0.111	0.257	2.330
60% Pt/C	0.394	0.753	2.408
Pt <sub>2</sub> Co/C	0.342	0.652	3.523
Pt <sub>3</sub> Co/C	0.160	0.260	0.510

Table 1: Peroxide yields (mole fraction) measured using a RRDE technique with a rotation rate of 900 rpm and various disk potentials of 0.7V, 0.6V, 0.4V Vs RHE in conjunction with a gold ring electrode polarized at 1.3V in 1M HClO<sub>4</sub> at room temperature.

Catalysts	WE @ 0.4 V		WE @ 0.6 V	
	$\sigma_{\text{after}} - \sigma_{\text{before}}$	$\eta_{\text{after}} - \eta_{\text{before}}$	$\sigma_{\text{after}} - \sigma_{\text{before}}$	$\eta_{\text{after}} - \eta_{\text{before}}$
	$\sigma_{\text{before}}$ (%)	$\eta_{\text{before}}$ (%)	$\sigma_{\text{before}}$ (%)	$\eta_{\text{before}}$ (%)
30% Pt/C	34	26	27	19
60% Pt/C	57	48	49	43
30% Pt <sub>2</sub> Co/C	50	40	44	34
30% Pt <sub>3</sub> Co/C	27	22	16	9

Table 2. Effect of cathode side durability tests with O<sub>2</sub>/N<sub>2</sub>, 40°C, 1 atm, for a duration of 24 hours using 30% Pt/C, 60% Pt/C, 30% Pt<sub>2</sub>Co, 30% Pt<sub>3</sub>Co at two different working electrode (WE) polarization potentials of 0.4 V and 0.6 V Vs DHE. Listed are the decreases in proton conductivity  $\sigma$  (S cm<sup>-1</sup>) and ion exchange capacity  $\eta$  (mEq g<sup>-1</sup>).

Cleavage of the side chain ether linkage (Fig. 3), which intrudes into the hydrophilic ionic cluster, is found to be the key initiator of conductivity and ion exchange capacity loss. Prolonged durability testing leads to breakage of certain sections of fluorocarbon backbone as observed in the stabilization of ion exchange capacity vs. a more linear decline in proton conductivity (Table 2). Normal operating cathode overpotentials of 0.6 and 0.7 V Vs RHE leads to lower membrane degradation relative to higher overpotentials of 0.4 V, this is directly correlated to peroxide yields measured

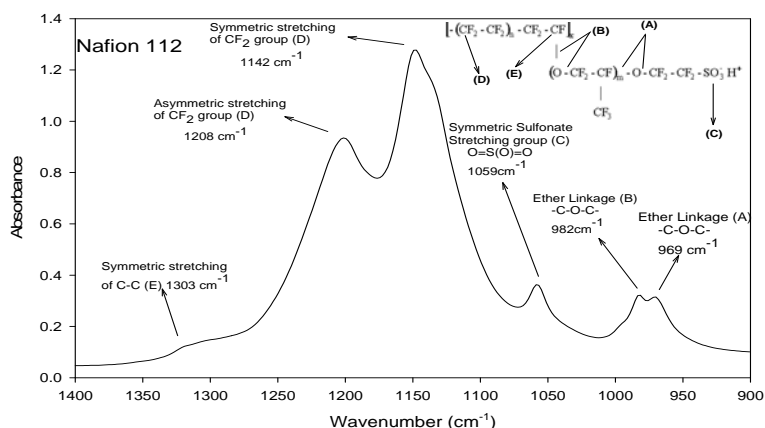


Figure 3: ATR-FTIR Spectrum of Nafion® 112 (H-form) indicating absorption bands obtained using ZnSe ATR crystal. [See text for references]

independently in RRDE. Higher the loading of catalyst on carbon support and corresponding larger the particle size results in higher peroxide yield and consequent higher membrane degradation as shown by the comparison between 60% Pt/C and 30% Pt/C used in this study. PtCo/C alloy catalyst with enrichment of surface Co gives lower

peroxide current and maintains lower level of membrane degradation as shown by the comparison between Pt<sub>2</sub>Co/C and Pt<sub>3</sub>Co/C. Temperature effects on membrane degradation was found to be linear with higher ORR activity and consequent higher peroxide generation at the interface. Degradation at the anode side due to oxygen crossover through the membrane was found to be insignificant relative to cathode side degradation within the duration of the experiments performed here. However these tests represent the narrow confines of interaction of absorbed hydrogen on Pt and its interaction with crossover oxygen.

## Fundamental Aspects of Ru Dissolution and Migration under DMFC Operating Environment

Student: Thomas Arruda (3<sup>rd</sup> year graduate student)

Postdoctoral Research Associate: Dr. Lajos Gancs (partial support)

In this work, we *explicitly* present the effect of Ru contamination on the ORR kinetics on Pt/C, in order to provide a link to PEMFC performance degradation. In our simplistic experimental approach, Ru was dissolved from a commercial unsupported PtRu electrocatalyst-based fuel cell electrode (referred as sacrificial electrode) directly into the liquid electrolyte, in which oxygen reduction was performed on a thin film Pt/C working electrode. Ru<sup>n+</sup> concentration was monitored using ICP-MS, while changes in ORR kinetics were addressed by rotating disk electrode experiments. A detailed study showing the Ru contamination under various fuel cell cathode operating conditions such as cathode overpotential, temperature and choice of electrocatalyst (Pt alloy vs. Pt) are presented in the full version of this report.

The kinetics of oxygen reduction on Pt/C can be explicitly followed up from the measured RDE current values after correcting for the mass transport-related contributions. The mass transport of oxygen at a pure Pt surface can be treated in a straightforward fashion since the surface is uniformly accessible to molecular oxygen at a given electrode potential. When the Pt surface is partially covered by Ru, the ORR activity becomes dependent on surface elemental composition due to the different reaction kinetics on the pure metals. Assuming that all Ru adatoms on Pt are oxidized and thereby inactive towards the adsorption of molecular oxygen at low ORR overpotentials (say at or

above 0.8 V), such a Pt-Ru bimetallic surfaces should perform like a pure Pt, albeit blocked by Ru to various extents<sup>2</sup>, unless the reaction mechanism changes (*vide infra*). Finding the electrochemical surface area for oxygen reduction at Pt-Ru electrodes however is a rather complicated task, it requires the exact knowledge of elemental composition and surface structure<sup>2</sup> as well as the adsorption energy of surface oxides at a given electrode potential<sup>3</sup>. Nevertheless, the blocking mechanism exerted by Ru is exactly what is analyzed here. This is attained by the comparison of the kinetic current values, which were calculated using Equation (1)<sup>4</sup>:

$$i_k = \frac{i_L \times i_m}{i_L - i_m} \quad (1)$$

$i_k$  was extracted from data corresponding to the mixed kinetics-mass transport region of the RDE polarization curve. We also mention that the current measured at 0.3 V ( $i_L$ ) is a pseudo-limiting current since the exposed Ru is partially covered by surface hydroxides at that electrode potential.

In Table 3, kinetic current density ( $j_k^*$ ) values are summarized which were obtained for clean and Ru-contaminated Pt/C electrode in 0.5 M H<sub>2</sub>SO<sub>4</sub>.  $j_k^*$  was calculated from  $i_k$  using and Equation (1) after normalizing it to the mass of Pt. Oxygen reduction is found to be at least 8-times more sluggish when the total number of dissolved Ru atoms is more than 3000-times higher than the number of surface Pt atoms, although the estimated Ru coverage of the Pt surface is less than 20 %. This is conceived based on a comparison of the amount of Ru present in a known concentration within the volume of the electrolyte and the number of Pt atoms exposed, as determined independently from ICP-MS data and from the H<sub>UPD</sub> area (from the cyclic voltammogram), respectively.

The Tafel pots in Figure 6 do not evidence any significant changes in the mechanism of oxygen reduction in the low overpotential region (between 0.8 V and 0.9V) upon Ru contamination as observed in H<sub>2</sub>SO<sub>4</sub>. For Pt/C in clean electrolyte, the Tafel slope was found -122 mV decade<sup>-1</sup>, which is quite close to those obtained for PtRu (-115 mV decade<sup>-1</sup>) and upon various Ru-contamination (-113 mV decade<sup>-1</sup>). This hints that at low ORR overpotential, oxygen reduction seems to proceed on the platinum sites exclusively, without the influence of other electrode reaction. The dramatic drop in ORR kinetics at Pt/C as a result of Ru contamination is readily evident from the Tafel-plots. In terms of overpotential, this can translate to a ca. 160 mV increase as the arrow

Table 3: Maximum possible ( $\Phi Ru^{max}$ ) and estimated actual ( $\Phi Ru^{est}$ ) Ru coverage levels on Pt/C and the corresponding Pt mass-specific kinetic current density ( $j_k^*$ ) values for ORR

	0.5 M H <sub>2</sub> SO <sub>4</sub>				1 M TFMSA	
$c_{Ru}^{n+}$ [ $\mu\text{mol dm}^{-3}$ ]	0	147	169	202	0	23
$\Theta_{Ru}^{max}$ [ML Pt]	0	2790	3210	3840	0	500
$\Theta_{Ru}^{est}$ [ML Pt]	0	0.12	0.18	0.31	0	0.14
0.90 V	28.59	20.27	3.55	3.42	39.32	23.11
$j_k^*$ [A cm <sup>-2</sup> g <sup>-1</sup> ]						
0.85 V	76.78	51.56	10.15	8.87	120.80	80.77
0.80 V	179.10	112.98	21.44	21.01	291.30	197.89

and also we consider here that Ru is in intimate contact with Pt in the PtRu electrocatalyst sample.

demonstrates in Figure 6. It is interesting to match the kinetic current values obtained for the Pt/C electrode in Ru-contaminated solutions to those measured for a PtRu electrocatalyst (Johnson & Matthey HiSpec6000) in clean electrolyte. For the PtRu electrocatalyst, we have estimated the initial Pt:Ru surface atomic composition to be 0.67 by copper underpotential deposition and subsequent removal<sup>5</sup>,

Furthermore, one can presume that above 0.85 V the Ru surface atoms are completely oxidized and thus do not reduce oxygen. Correcting for a surface blocking factor of 0.43 due to a inactive higher Ru oxidation state, indeed similar kinetic current values could be calculated in the clean electrolyte for both Pt/C and PtRu at low ORR overpotentials. However, several fold lower kinetic current values were measured for the Pt/C electrode when the  $\text{Ru}^{n+}$  concentration exceeded  $150 \mu\text{mol dm}^{-3}$  as compared to those obtained for the Pt:Ru electrocatalyst in clean electrolyte. The CV data showing  $H_{\text{upd}}$  based electrochemically active surface area ascribed to Pt sites, is contrary to the above observations on the basis of Ru atoms present on the surface (Table 1). This is exemplified on the basis of the Cu upd measurements of Ru presence on PtRu electrocatalyst where surface coverage of 43 atom percent is reported. The blocking effect of Pt/C in  $\text{Ru}^{n+}$  solutions was significantly lower (Table 1) when compared in electrolyte containing different  $\text{Ru}^{n+}$  concentrations. This apparent discrepancy is explained by taking into account the nature of Ru accumulation on Pt in the atomic level. Namely, Ru is expected to reach higher coverage levels on Pt according to the Volmer-Weber growth mechanism, *viz.* by the formation of three-dimensional clusters with heights of several atomic layers.<sup>6</sup> For such electrode structures, the transport and reduction of oxygen can be limited to the topmost Ru atoms while the underlying Pt sites might be less utilized. In other words, the electrode blocking factor is higher than what can be calculated from the ratio of Ru-covered Pt/C and the clean Pt/C  $H_{\text{UPD}}$ . (Note that the  $H_{\text{upd}}$  area does not reflect the transport of dissolved oxygen.) This

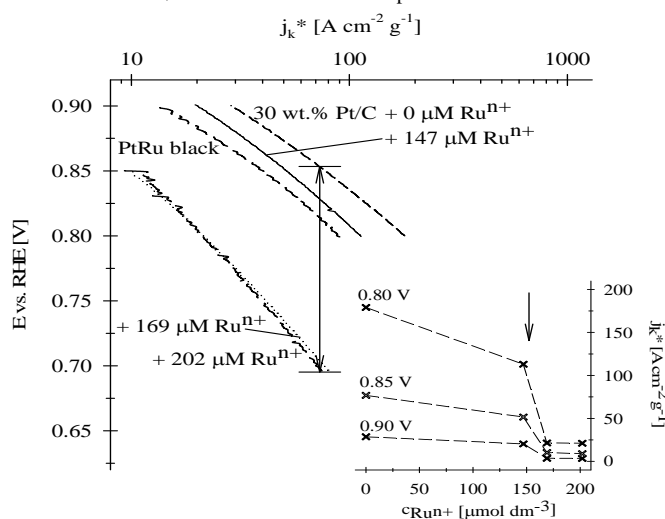


**Figure 4.** Mass transport-corrected Tafel plots for oxygen reduction on a thin film 30 wt. % Pt/C,  $0.28 \text{ cm}^2$ ,  $15 \mu\text{g}_{\text{Pt}} \text{ cm}^{-2}_{\text{GC}}$  and PtRu black electrode in  $\text{O}_2$ -saturated  $0.5 \text{ mol dm}^{-3} \text{ H}_2\text{SO}_4$  solution containing dissolved Ru species in various concentrations. The inset shows the corresponding changes to the mass-specific kinetic current densities of oxygen reduction on Pt as a function of Ru concentration of the electrolyte at three electrode potentials.

simplistic model can explain why the ORR activity diminishes progressively on Pt as a function of  $\text{Ru}^{n+}$  concentration and why the contaminated electrode behaves just as a pure Ru electrode beyond a threshold concentration<sup>7</sup> (see inset in Figure 6). A detailed investigation of the dynamics of Ru ad-layer formation as a function of electrode potential with and without the presence of dissolved oxygen is currently in progress.

### Fundamental understanding of anion adsorption on Pt and Pt alloy electrocatalysts. Thomas Arruda, Nagappan Ramaswamy (2<sup>nd</sup> year graduate students)

Since Halide anion adsorption on Pt was first described by Slygin in 1935, many studies have been published. Early work probing the effects of anions on hydrogen underpotential deposition ( $H_{\text{upd}}$ ) on Pt suggested low concentrations of Halide anions significantly change  $H_{\text{upd}}$  peaks with respect to potential and magnitude. Other investigators have concentrated their efforts to higher potentials where oxygen reduction reaction (ORR) is expected to take place. In more recent efforts rotating ring disk experiments (RRDE) showed that even trace levels (as low as  $10^{-4} \text{ M}$ ) of  $\text{Cl}^-$  significantly altered the Pt cyclic voltammogram (CV) and produced large quantities of  $\text{H}_2\text{O}_2$ .

Others have attempted to understand anion adsorption by structural elucidation of the adlayer on the surface. Surface sensitive techniques utilized include Auger Electron Spectroscopy (AES), Low Energy Electron Diffraction (LEED), and Surface X-Ray Scattering (SXS). An AES/LEED study indicated that  $\text{Cl}_{\text{ads}}$  occurred on the Pt(100) facet at lower electrode potentials than on Pt(111), suggesting that Pt(100) is more susceptible to poisoning. One common thread in the aforementioned techniques though is the necessity for an ultra high vacuum (UHV) environment. In addition, the previous studies have been performed on single crystal materials. In order to understand fuel cell relevant surface/adsorbate interactions, it is desirable to utilize *in situ* techniques on actual fuel cell catalysts. In their reports, Marković *et al.* used *in situ* SXS to probe the interaction of Pt particles with Halide anions. Surface coverage and adlayer structural information was obtained, but only on Pt(111) single crystals.

Figure 5 shows the resulting  $\Delta\mu$  curves for Pt/C in clean 1M  $\text{HClO}_4$ , and the corresponding solutions contaminated with 1 and 10mM KCl. Figure 5a represents “water activation” as it occurs on Pt/C in 1M  $\text{HClO}_4$  and agrees well with previously reported data. All of the data sets contain a sinusoidal line shape at 0.24V indicating a strong presence of adsorbed hydrogen ( $\text{H}_{\text{ads}}$ ). In addition to a clear increase in  $\Delta\mu$  peak intensity, there is a corresponding “shift” in peak position which has been attributed to a change in  $\text{O}[\text{H}]_{\text{ads}}$  binding site from atop to n-fold as the electrode potential is increased. The  $\Delta\mu$  curves in Figure 5b show a systematic increase in peak intensity however, there is a lack of peak shift as they are already situated at higher absorption energy ( $\sim 5\text{eV}$  in respect to the edge). This suggests that any  $\text{Cl}_{\text{ads}}$  present impedes the formation of lower coordinated Pt-O[H] geometries (atop/bridged), thus forcing O[H] directly into 3-fold sites. Figure

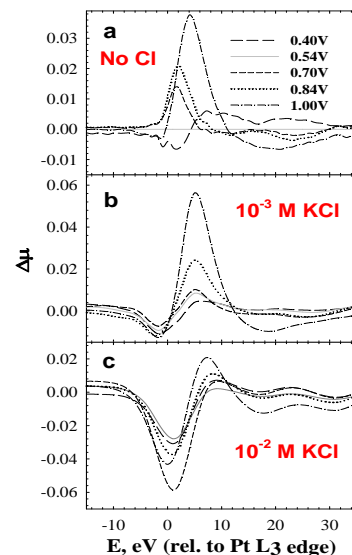


Figure 5. Pt  $\text{L}_3$  edge  $\Delta\mu = \mu(\text{V}) - \mu(0.54\text{V clean})$  spectra as a function of electrode potential in (a) 1M  $\text{HClO}_4$  (clean), (b) 1M  $\text{HClO}_4 + 1\text{mM KCl}$  and (c) 1M  $\text{HClO}_4 + 10\text{mM KCl}$ . The peak

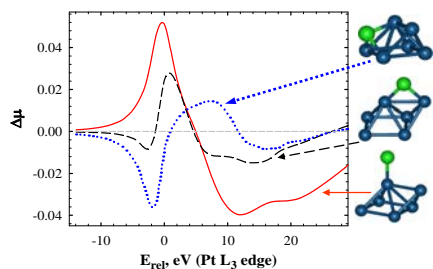


Figure 6. Theoretical  $\Delta\mu$  signatures (non shifted, scaled) calculated by FEFF8.0,  $\Delta\mu = \mu(\text{Pt}_6\text{-Cl}) - \mu(\text{Pt}_6)$  for (a) atop Cl, (b) bridged Cl and (c) 3-fold Cl (fcc site).

5c features a large minima ( $\sim 0\text{eV}$ ) as well as a suppressed maxima in the  $\text{O}[\text{H}]_{\text{ads}}$  region of the  $\Delta\mu$  spectrum with little variation as the electrode potential is increased. Both the large negative peak, and the low intensity  $\text{O}[\text{H}]$  peak suggests a strong presence of  $\text{Cl}_{\text{ads}}$  at all potentials. Fitting of the experimental  $\Delta\mu$  curves was performed by comparison to theory calculations from FEFF8.0. Figure 6 shows the FEFF8.0 calculated  $\Delta\mu$  line shapes (not shifted or scaled) with corresponding depictions of the  $\text{Pt}_6$  cluster and adsorbed Cl with a Pt-Cl distance of  $2.4\text{\AA}$ . The solid line representing atop  $\text{Pt}_6\text{-Cl}$  contains a large maxima near the edge position followed by significant negative contribution. This line shape has not been found in the experimental data, indicating the absence of atop Pt-Cl. The dashed line representing bridged Cl resembles the line shape found in 1mM  $\text{Cl}^-$ , suggesting that at 1mM  $\text{Cl}^-$  concentration,  $\text{Cl}_{\text{ads}}$  occurs in a 2-fold configuration. This result is consistent with the lack of peak shifting found in Figure 5b. By assuming that the bridged site is occupied by  $\text{Cl}_{\text{ads}}$ , it is evident that  $\text{O}[\text{H}]_{\text{ads}}$  becomes hindered until the potential is high enough for it to directly adsorb 3-fold. The FEFF calculated  $\Delta\mu$  for 3-fold  $\text{Cl}_{\text{ads}}$  in Figure 6 (dotted line) compares closely with the experimental  $\Delta\mu$  line shape for 10mM  $\text{Cl}^-$ , especially noting the large minima followed by a small positive peak. This result implies that  $\text{Cl}_{\text{ads}}$  occurs 3-fold at 10mM and is further supported by a lack of 3-fold  $\text{O}_{\text{ads}}$  (intense maxima in Figure 5a)



signature in the experimental  $\Delta\mu$  spectra. The reason for a change from bridged to 3-fold with a 10 fold increase in  $\text{Cl}^-$  concentration is still unclear however.

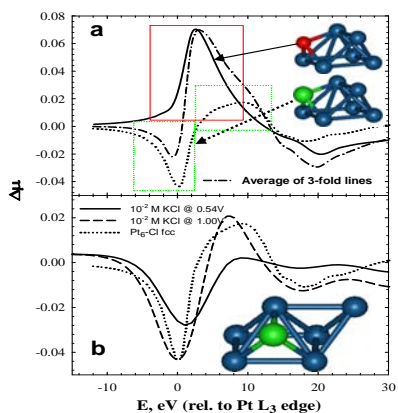


Figure 7. (a) Comparison of theoretical 3-fold O (solid) and 3-fold Cl (dotted)  $\Delta\mu$  signatures. The dash-dot line shows the sum of the two curves. (b) Comparison of experimental  $\Delta\mu$

signatures. The dash-dot line, showing the sum of 3-fold  $\Delta\mu$  theory exhibits an astonishing likeness to the experimental data in  $10^{-3}$  M chloride. This is, in our opinion, the best evidence indicating 3-fold chloride adsorption occurring in parallel with 3-fold O[H] formation.

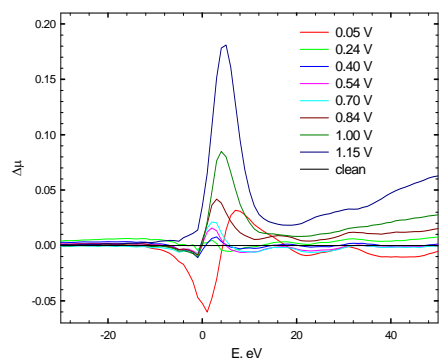


Figure 9: Experimental  $\Delta\mu$  signatures obtained at Pt  $L_3$  edge in deoxygenated 0.1M  $\text{HClO}_4$  electrolyte with 10 mM HBr as poison

In the case of  $10^{-3}$  M chloride the adsorption geometry is not as obvious as it was in  $10^{-2}$  M  $\text{Cl}^-$ . The theoretical  $\Delta\mu$  line shapes suggest bridge bonded adsorption; however, we interpret the spectra to be a combination of  $\text{H}_2\text{O}$  activation (hence presence of surface oxides) and 3-fold  $\text{Cl}^-$  adsorption occurring concurrently. There is direct evidence of both chloride and O[H] adsorption in the  $\Delta\mu$ . To illustrate this, Figure 7a shows the FEFF 8.0  $\Delta\mu$  simulations for 3-fold O and 3-fold  $\text{Cl}^-$  with boxes to emphasize the major elements of each adsorbing species. Both  $\text{Pt}_6$  clusters show 3-fold adsorption of chloride and O[H] with vastly different  $\Delta\mu$  signatures. The dash-dot line, showing the sum of 3-fold  $\Delta\mu$  theory exhibits an astonishing likeness to the experimental data in  $10^{-3}$  M chloride. This is, in our opinion, the best evidence indicating 3-fold chloride adsorption occurring in parallel with 3-fold O[H] formation.

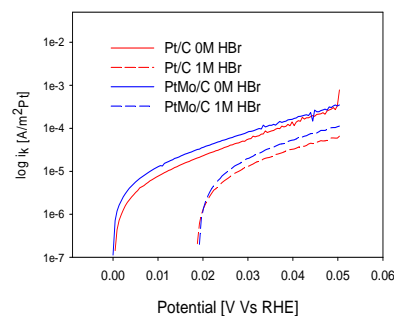


Figure 8: Tafel plots for HOR showing the activity of Pt and PtMo electrocatalysts in 0.1M  $\text{HClO}_4$  electrolyte with and without 1M HBr as poison

A similar effort but with technological impact is also underway in our laboratory. This involves the development of electrocatalysts  $\text{H}_2$  oxidation/evolution (HOR/HER) in for application in  $\text{H}_2$ - $\text{Br}_2$  hybrid flow battery. The challenge here involves development of electrocatalyst for (HOR/HER) reaction that is also tolerant to bromide anion poisoning. Typical electrolyte used in this hybrid flow battery system is 3M HBr. Figure 8 shows the HOR activity of in house developed carbon supported PtMo in comparison to Pt/C without and without 1M HBr as the poison in deoxygenated 0.1M  $\text{HClO}_4$ . This indicates the superior tolerance of PtMo electrocatalyst in comparison to Pt/C. Our novel  $\Delta\mu$  is being used in order to understand the site specific adsorption properties of bromide anions on Pt and PtMo electrocatalysts to elucidate the possible differences between Pt and PtMo as HOR electrocatalysts in the presence of bromide anions.

## References

- (1) Zhang, L.; Mukerjee, S. *Journal of The Electrochemical Society* **2006**, *153*, A1062.
- (2) Treimer, S.; Tang, A.; Johnson, D. C. *Electroanalysis* **2002**, *14*, 165.
- (3) Markovic, N. M.; Ross, P. N. *Surface Science Reports* **2002**, *45*, 117.
- (4) Murthi, V. S.; Urian, R. C.; Mukerjee, S. *Journal of Physical Chemistry B* **2004**, *108*, 11011.
- (5) Ganes, L.; Hakim, N.; Hult, B.; Mukerjee, S. Dissolution of Ru from PtRu Electrocatalysts and its Consequences in DMFCs. In *ECS Transactions Volume 3, Proton Exchange Membrane Fuel Cells 6*; Fuller, T., Bock, C., Cleghorn, S., Gasteiger, H. A., Jarvi, T. D., F., M. M., Murthy, M., V., N. T., Ramani, V., Stuve, E. M., Zawodzinski, T., Eds.; The Electrochemical Society, Inc.: Pennington, NJ, 2006; pp 607.

- (6) Spendelow, J. S.; Babu, P. K.; Wieckowski, A. *Current Opinion in Solid State & Materials Science* **2006**, 9, 37.
- (7) Cao, D.; Wieckowski, A.; Inukai, J.; Alonso-Vante, N. *Journal of the Electrochemical Society* **2006**, 153, A869.